JOURNAL OF NEUROPHYSIOLOGY

J Neurophysiol 128: 239–248, 2022.
First published June 29, 2022; doi:10.1152/jn.00091.2022

RESEARCH ARTICLE

Higher Neural Functions and Behavior

Facilitation and inhibition effects of anodal and cathodal tDCS over areas MT+ on the flash-lag effect

Wu Wang,[1] Xiao Lei,[2] Wenxiao Gong,[1] Kun Liang,[1] and Lihan Chen[1]

[1]*School of Psychological and Cognitive Sciences and Beijing Key Laboratory of Behavior and Mental Health, Peking University, Beijing, People's Republic of China and* [2]*Academy for Advanced Interdisciplinary Studies, Peking University, Beijing, People's Republic of China*

Abstract

The perceived position of a moving object in vision entails an accumulation of neural signals over space and time. Due to neural signal transmission delays, the visual system cannot acquire immediate information about the moving object's position. Although physiological and psychophysical studies on the flash-lag effect (FLE), a moving object is perceived ahead of a flash even when they are aligned at the same location, have shown that the visual system develops the mechanisms of predicting the object's location to compensate for the neural delays, the neural mechanisms of motion-induced location prediction are not still understood well. Here, we investigated the role of neural activity changes in areas MT+ (specialized for motion processing) and the potential contralateral processing preference of MT+ in modulating the FLE. Using transcranial direct current stimulations (tDCS) over the left and right MT+ between pre- and posttests of the FLE in different motion directions, we measured the effects of tDCS on the FLE. The results found that anodal and cathodal tDCS enhanced and reduced the FLE with the moving object heading to but not deviating from the side of the brain stimulated, respectively, compared with sham tDCS. These findings suggest a causal role of area MT+ in motion-induced location prediction, which may involve the integration of position information.

NEW & NOTEWORTHY Perceived positions of moving objects are related to neural activities in areas MT+. We demonstrate that tDCS over areas MT+ can modulate the FLE, and further anodal and cathodal tDCS facilitated and inhibited the FLE with a moving object heading to but not deviating from the side of the brain stimulated, respectively. These findings suggest a causal role of area MT+ in motion-induced location prediction and contribute to understanding the neural mechanism of the FLE.

area MT+; facilitation; flash-lag effect; inhibition; tDCS

INTRODUCTION

The ability to accurately localize moving objects in the environment is crucial for our daily lives (1–3). Signal processing for moving objects from the retina to the visual cortex needs time. When the signal reaches the cortical areas specialized for motion processing, the moving object has already changed to different positions. Thus, signals in motion processing cortex (e.g., the lateral occipitotemporal cortex, MT+) are already outdated (4–6). To compensate for the delays during neural transmission, the visual system might apply the previous trajectory of a moving object to predict the object's location in the current moment (5, 7, 8). Therefore, the perceived spatial location of a moving object appears to be shifted forward in the direction of its motion, relative to its physical location (3, 9). Although physiological and psychophysical studies on motion-induced location shift have been documented (2, 4–6, 8, 10), its underlying neural mechanisms are not well understood.

The illusory shift of a perceived position has been extensively verified using the flash-lag effect (FLE), in which a moving object is perceived ahead of a static flash even when physically aligned with the moving object. Ever since the effect was proposed, scientific debates on the effect have still lasted (4–6, 8). Proposed mechanisms contain visual attentional shifting between moving targets and flashes (11, 12), differential latencies for the neural

Correspondence: L. Chen (clh@pku.edu.cn).
Submitted 7 March 2022 / Revised 21 June 2022 / Accepted 22 June 2022

processings of moving and static objects (13), the average position of a moving object over a certain time (14), postdictive assignments of the post-flash positions to the moment of flashes (15), and predictive assignments of perceived positions (8, 16). Despite the contradictions among the various psychophysical mechanisms, it appears to be gradually realized that none of the mechanisms could singly interpret all of the rich FLE phenomena (4, 6, 17). One common conception of most mechanisms is that motion perception intricately links with position perception (9, 18). However, it is unclear whether modulation of neural activation in cortical areas selectively processing motion could affect motion-induced position mislocalization. Although one study has found the reduced FLE due to neural disruption in area MT+ (4), the neural processes underlying the causal contribution of area MT+ to the FLE are poorly understood.

Area MT+ plays a central role in visual motion processing (19, 20). Neuroimaging studies have found motion perception deficits in patients with brain damage localized to MT+ (21, 22). And transcranial magnetic stimulation (TMS) studies of MT+ observed visual motion perception impairment (22–25). Interestingly, MT+ shows preferential motion processing and attention to motion in the contralateral visual field (21, 22, 26), although it could potentially integrate motion in the left and right hemifields (25, 27). The motion processing preference of MT+ might result from an MT+ subregion (MT) (22, 26), whose receptive field (RF) extends a much lesser degree to the ipsilateral visual field (28) and response is selective to translational motion (29). Furthermore, MT+ also engages the perceived position of a static object after motion adaptation (30, 31). As the FLE involves the integration of signals for the perceived positions of the static and moving objects, the neural activation changes of MT+ due to transcranial direct current stimulation (tDCS) could modulate the FLE. Therefore, our aim is to test how tDCS over MT+ modulates the FLE.

tDCS, a noninvasive electrical-stimulating technique, has been shown to modulate the excitability of MT+. Generally, anodal stimulation (a-tDCS) increases cortical excitability by depolarization, whereas cathodal stimulation (c-tDCS) decreases it by hyperpolarization (32, 33). Nevertheless, the modulation of neural activity by tDCS is more complicated than the expectation (34), thereby exhibiting inconsistent modulation effects. For instance, c-tDCS on the left MT+ enhanced complex motion (low coherence) perception and worsened simple movement (high coherence) perception (35); a-tDCS on the left MT+ enhanced motion direction identification ability (36); both a- and c-tDCS on the left MT+ improved coherent motion discriminability in the right hemifield (33). These contradictory findings might suggest an interaction of tDCS modulation effects with task characteristics (33, 37). Although tDCS on MT+ indeed modulated motion perception, it is little known how a- and c-tDCS on the left and right MT+ affect the FLE. In addition, due to the possible contralateral processing preference of MT+ (22, 26, 29), the stimulated areas (the left vs. the right MT+) might lead to various modulation effects of tDCS over MT+ on the FLE. Therefore, our final aim is to estimate how a- and c-tDCS on the left and right areas MT+ enhance and impair the FLE in different motions (e.g., from the right to the left and the left to the right cross the vertical meridian).

To address the questions mentioned earlier, we applied the standard visual FLE. In *experiment 1*, we aimed to explore the modulation effects of a- and c-tDCS over the left MT+ on the FLE in different motion directions. Thus, three participant groups were assigned to different stimulation regimes (anodal vs. cathodal vs. sham) to perform two sessions of the flash-lag tasks with 15-min intervals of tDCS. By comparing the FLE magnitudes in different motion directions between two sessions in each group, we assessed the facilitation and inhibition effects of a- and c-tDCS over the left MT+ on the FLE. In *experiment 2*, we further tested the modulation effects of a- and c-tDCS over the right MT+ on the FLE in different motion directions. All experimental conduction was the same as that in *experiment 1*, except for the stimulated area (the right MT+). By comparing the FLE magnitudes in different motion directions between two sessions in each group, we estimated the similar effects of a- and c-tDCS over the right MT+ on the FLE.

MATERIALS AND METHODS

Experiment 1: Effects of tDCS over the Left MT+ on the FLE

Participants.

A total of 45 healthy volunteer undergraduate and graduate students were recruited to join *experiment 1*. They all reported normal or corrected-to-normal visual acuity, no metallic implants, and no prior history of any neurological or mental illnesses, drug abuse, or drunkenness. Participants were naïve to the purpose of the experiment and were randomly and equally assigned to three experimental groups: anodal group (aged 18–23 yr, mean 19.9 ± 1.55 yr; 8 females; 5 left-dominated eye; all right-handedness), cathodal group (aged 18–21 yr, mean 19.1 ± 1.10 yr; 9 females; 1 left-dominated eye; all right-handedness), and sham group (aged 18–24 yr, mean 20.0 ± 1.96 yr; 10 females; 3 left-dominated eye; 2 left-handedness). Each group performed two sessions of the flash-lag tasks with 15-min intervals of tDCS. All participants gave written informed consent. The testing procedures were approved by the Academic Affairs Committee of the School of Psychological and Cognitive Sciences of Peking University.

Transcranial direct current stimulation.

We applied a battery-driven stimulator (Brain Premier E1) to deliver constant current. A pair of rubber electrodes with each an ~19.6 cm^2 saline-soaked synthetic sponge was used for current delivery. For the anodal stimulation, one anodal electrode was put over the left MT+ that was located 2.5 cm above and 5 cm left of the inion (4, 33); the other cathodal electrode was positioned over the central parietal lobe (Cz, the intersection of the nasion-inion line and left-right preauricular recess line, according to the international 10–20 EEG system) (35, 38). For the cathodal stimulation, the cathodal and anodal electrodes were reversely placed. In the present study, the current with an intensity of 1.5 mA was used for 15 min, with a 1.5 mA/19.6 cm^2 dose current density. During the stimulation, the current was ramped on 1.5 mA within 15–30 s.

Stimulus presentation.

Under the environment of MATLAB (2020a, The MathWorks, Natick, MA), we used Psychtoolbox-3 to present all visual stimuli on a color monitor [27-in. (68.58 cm) DP with a frame rate of 100 Hz] controlled by a personal computer (39, 40).

Stimuli and the flash-lag task.

Stimuli consisted of a white fixation cross, a black bar (2° × 0.6°), and a small white circle (diameter = 0.6°). As is shown in Fig. 1*A*, the white fixation cross was always visible at the center of the screen against a gray background [RGB (80 80 80)] throughout a session. The black bar was randomly displayed at either the right or the left of the screen. At the beginning of each trial, the center of the bar was initially put 6.67° above and 7° to the right or the left of the fixation cross. After its appearance, the bar immediately moved toward the opposite side of the screen. As the frame-to-frame spatial offset was 0.1°, the constant and smooth speed of the bar was 10°/s. The small white circle, whose diameter was equal to the width of the bar, was flashed 6.67° above the fixation cross for one refresh frame (10 ms). When the bar crossed the center of the screen, the circle flashed at different timings (−6, −4, −2, 0, 2, 4, and 6 refresh cycles of the monitor, or −60 ms to 60 ms) so that it appeared at various locations relative to the bar.

Task procedure.

Participants were seated in a dark room and viewed binocularly the screen from a distance of 60 cm, with their heads placed on a chin tray. Throughout a trial, they fixated on the white fixation cross. Then the bar appeared and moved to the opposite side, when the white circle was flashed, participants were asked to indicate its position relative to the bar (the left or right). Thus, the task was an unspeeded and two-alternative forced-choice response. In 1 s after the response, the next trial began. To avoid the expectance effect of the flashed circle, we added two perturbation conditions where the initial positions of both the small white circle and the bar were shifted by the left and right 0.5° relative to the white

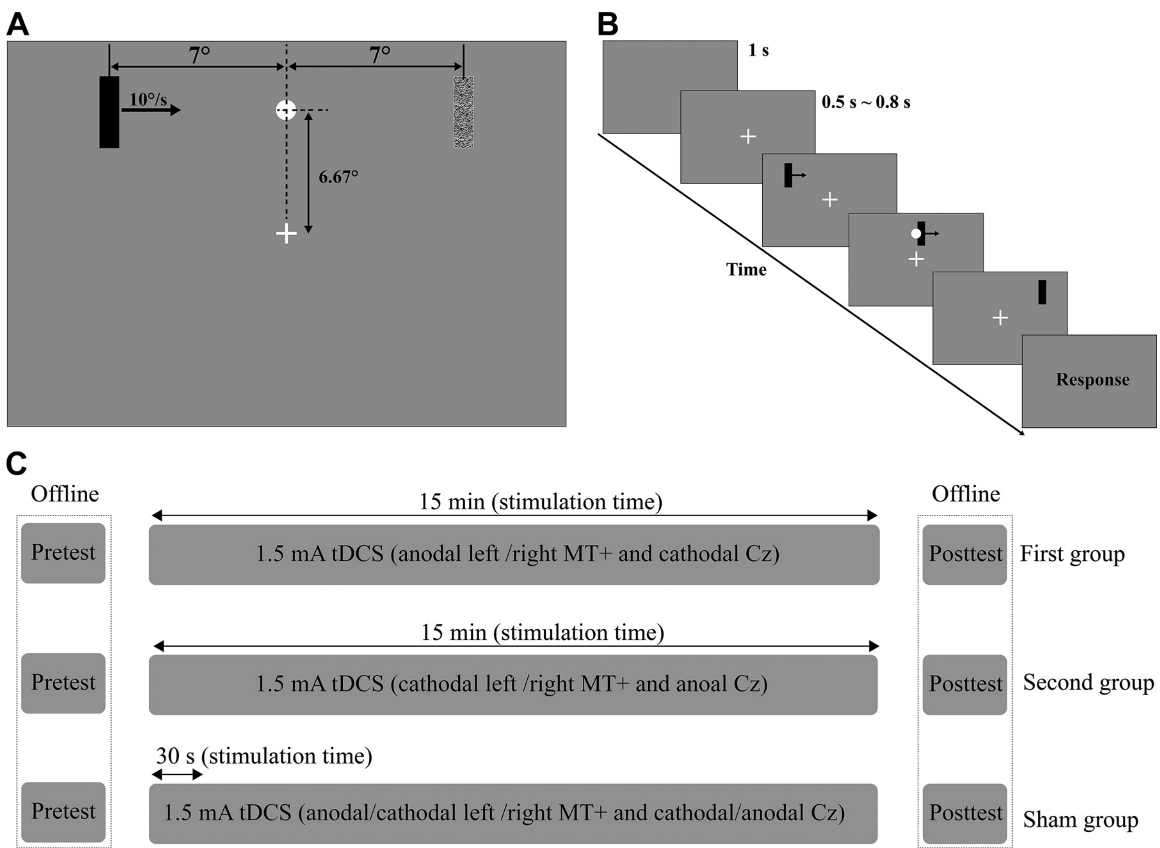

Figure 1. Depictions of stimulus displays, an example of one trail of the flash-lag task, and experimental setups for the anodal, cathodal, and sham stimulation. *A*: depictions of stimulus displays. Stimuli contain a white fixation cross, a black bar (2° × 0.6°), and a small white circle (diameter = 0.6°). The black bar is randomly displayed at either the right (position with a rectangle texture) or the left of the screen. *B*: an example of one trail of the flash-lag task. During one trial of the flash-lag task, the participant fixates on the white fixation, after 0.5–0.8 s, the black bar appears on one side of the screen and immediately moves toward the opposite side. During the movement of the bar, the small white circle is flashed above the fixation cross for one refresh frame at different timings. When the bar moves to the terminal and disappears, the participant is indicated to report the relative positions of the circle and the bar. If they perceive that the flashed circle is located on the left relative to the bar, they press the left button of a mouse; if they perceive that the flashed circle is located on the right relative to the bar, they press the right button of the mouse; if they perceive that the flashed circle completely coincides with the bar in space, they have to make an arbitrary choice. In 1 s after the response, the next trial begins. *C*: the experimental setups for the anodal, cathodal, and sham stimulation with different electrodes. Each group performed two sessions (pre- and posttests) of the flash-lag task under an offline condition. Between sessions, each group received the correspondent current stimulation. Cz, central parietal lobe; tDCS, transcranial direct current stimulations.

fixation cross. In addition to seven various timings of the flashed circle, we applied randomly a repetition of 21 trials for each timing. Therefore, the block from the right to the left motion consisted of 147 trials, and so did the block from the right to the left motion. Finally, a session, including the two blocks, consisted of 294 trials and lasted ~15 min. Before the formal experiment, we provided a practice block of 42 trials that traversed all conditions.

Study protocol.

We applied a randomized single-blind design to assign the participants into three experiment groups (anodal vs. cathodal vs. sham). Each group performed two sessions (pre- and posttests) of the flash-lag task. Between sessions, the anodal group received the anodal stimulation. Two elastic headstraps were used to fix the anodal electrode over the left MT+ and the cathodal electrode over the Cz. After the fixation of the electrodes, the participants received the current with an intensity of 1.5 mA for 15 min; for the cathodal group, they received the same current with the cathodal electrode over the left MT+ and the anodal electrode over the Cz; for the sham group, participants received the same current for 30 s, after that the current was turned off (Fig. 1*C*). In addition, we used a tool (ROAST) to model the normal component of the electrical field (V/m) created by the montage targeting the left MT+ (see Fig. 2, *left*); each intensity is represented by the different values on the heatmap (41, 42).

Data processing and analysis.

To estimate the magnitude of the FLE, we applied the logistic curve as used in previous studies (43–46). The following is the equation:

$$y = \frac{1}{1 + e^{\alpha + \beta x}}.$$

There are two critical parameters in the equation: α and β. −α/β represents the *x*-value of the sigmoid curve midpoint, and β indicates the logistic growth (slope). The participant's responses were transferred to a cumulative normal distribution, and then we applied the least square method to fit a logistic curve. We defined the timing point at accuracy rates of 50% as the magnitude of the FLE, namely, the point of subjective equality (PSE). And the just noticeable difference (JND) was defined as half of the difference between the timing points at accuracy rates of 25% and 75% in a coordinate. We did two-way repeated-measures ANOVA using the bruceR function in R programming (47), with the Bonferroni correction for multiple comparisons.

RESULTS

To estimate the effects of tDCS on the left area MT+ on the FLE in different motion directions, we performed a 2 (testing: pretest vs. posttest) × 2 [motion direction: the right to the left (RL) vs. the left to the right (LR)] repeated-measures ANOVA with the PSE as the dependent measure in anodal, cathodal, and sham groups, respectively (see Supplemental Material; https://doi.org/10.6084/m9.figshare.19187522.v1). For the anodal group, we observed a significant testing × motion direction interaction effect ($F_{1,14}$ = 10.38, $P < 0.01$, η_p^2 = 0.43) (Fig. 3*A*). A simple interaction analysis indicated that the posttest PSE was lower than the pretest PSE in the RL motion direction (t_{14} = 3.72, $P < 0.01$, Cohen's d = 0.64) (Fig. 3*A*). For the cathodal group, we observed a significant main effect of testing ($F_{1,14}$ = 15.45, $P < 0.01$, η_p^2 = 0.53) and a significant testing × motion direction interaction effect ($F_{1,14}$ = 12.87, $P < 0.01$, η_p^2 = 0.44) (Fig. 3*B*). A simple interaction analysis indicated that the prettest PSE was lower than the posttest PSE in the RL motion direction (t_{14} = 5.82, $P < 0.01$, Cohen's d = 1.12), and posttest PSE in the RL motion direction was higher than that in the LR motion direction (t_{14} = 2.28, $P < 0.05$, Cohen's d = 0.66) (Fig. 3*B*). For the sham group, no significant results were found (Fig. 3*C*). For three groups, the JNDs did not significantly differ across different testings and motion directions (see Supplemental Fig. S1).

To avoid the individual difference and better verify the effects of tDCS on the FLE in the RL motion direction, we normalized pre- and posttests of the PSE in each group using a min-max normalization method (linearly transforming x to y = (x-min)/(max-min), where min and max are the minimum and maximum values in pre- or posttests of the PSE, where x is the set of observed values of pre- or posttest PSEs) (48). Then, we run a 2 (testing: pretest vs. posttest) × 2 (stimulation: anodal vs. cathodal vs. sham) repeated-measures ANOVA with the normalized PSE as the dependent measure. We observed a significant testing × stimulation interaction effect ($F_{2,42}$ = 17.01, $P < 0.01$, η_p^2 = 0.45) (Fig. 3*D*). A simple interaction (Bonferroni correction) analysis indicated that

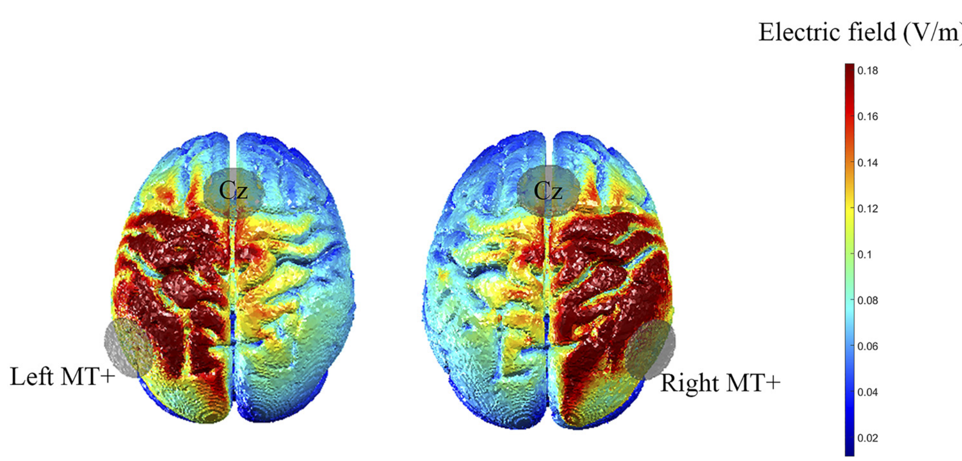

Figure 2. Current electrical field model. Modeling of the normal component of the electrical field (V/m) created by the montage targeting the left MT+ (*experiment 1*) and right MT+ (*experiment 2*); each intensity is represented by the different values on the heatmap. The same dispersion of current (1.5 mA) was outputted for each intensity value represented on a standardized head; ROAST MNI152 head (41, 42).

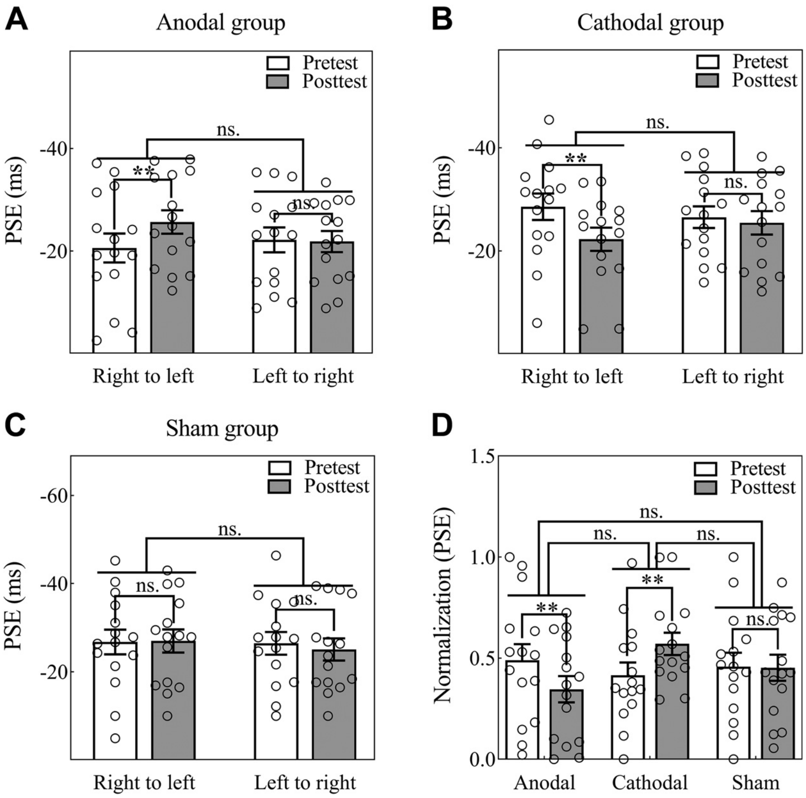

Figure 3. Effects of transcranial direct current stimulations (tDCS) over the left MT+ on the flash-lag effect (FLE) in different motion directions. *A*: effects of anodal (a)-tDCS. The pretest point of subjective equality (PSE) is significantly higher than the posttest PSE in the right to the left (RL) motion direction; the pretest PSE is nearly equal to the posttest PSE in the left to the right (LR) motion direction. *B*: effects of cathodal (c)-tDCS. The pretest PSE is significantly lower than the posttest PSE in the RL motion direction; the pretest PSE is nearly equal to the posttest PSE in the LR motion direction. *C*: effects of the sham tDCS. There are no significant results; the test PSEs are nearly equal. *D*: effects of tDCS over the left MT+ on the FLE in the RL motion direction. To avoid the individual difference and better verify the effects of tDCS on the FLE in the RL motion direction, we normalized pre- and posttests of the PSE in each group using a min-max normalization method. The normalized pre- and posttest PSEs in three types of stimulations do not significantly differ, respectively; in the anodal stimulation, the normalized pretest PSE is significantly higher than the normalized posttest PSE; in the cathodal stimulation, the normalized pretest PSE is significantly lower than the normalized posttest PSE. Hollow circles represent individual points in each group. $**P < 0.01$; ns, nonsignificant.

the normalized pretest PSE was higher than the normalized posttest PSE in the anodal stimulation (t_{42} = 4.17, $P <$ 0.001, Cohen's d = 1.10), the normalized pretest PSE was lower than the normalized posttest PSE in the cathodal stimulation (t_{42} = 4.07, $P <$ 0.001, Cohen's d = 1.08) (Fig. 3*D*).

To further verify the increased effect of tDCS on the FLE in the LR motion direction, we run a 2 (testing: pretest vs. posttest, within-group) × 2 (stimulation: anodal vs. sham, between-group) mixed-model ANOVA with the PSE as the dependent measure (49). We observed a significant testing × stimulation interaction effect ($F_{1,28}$ = 4.90, $P <$ 0.05, η_p^2 = 0.15) (Fig. 4*A*). A simple effect analysis indicated that the pretest PSE was higher than the posttest PSE in the anodal stimulation (t_{28} = 3.28, $P <$ 0.01, Cohen's d = 0.86), and no other significant results were found. Furthermore, we compared the discrepancy of increase effect between anodal and sham groups. The increase in PSE (posttest – pretest) was estimated via the independent sample t test (two-tailed), with the result indicating that the increased effect in the anodal group was more than that in the sham group (t_{28} = 2.21, $P <$ 0.05, Cohen's d = 0.81) (Fig. 4*B*). Likewise, we further confirmed the decreased effect of tDCS on the FLE in the RL motion direction, we run a 2 (testing: pretest vs. posttest, within-group) × 2 (stimulation: cathodal vs. sham, between-group) mixed-model ANOVA with the PSE as the dependent measure. We observed a significant testing × stimulation interaction effect ($F_{1,28}$ = 12.22, $P <$ 0.01, η_p^2 = 0.15) (Fig. 4*C*). A simple effect analysis indicated that the pretest PSE was lower than the posttest PSE in the cathodal stimulation (t_{28} = 4.79, $P <$ 0.001, Cohen's d = 1.26), and no other significant results were found. Furthermore, we compared the discrepancy of the decreased effect between cathodal and sham groups. The decrease in PSE (posttest − pretest) was estimated via the independent sample t test (two-tailed), with the result indicating that the decreased effect in the cathodal group was more than that in the sham group (t_{28} = 3.50, $P <$ 0.01, Cohen's d = 1.28) (Fig. 4*D*).

Experiment 2: Effects of tDCS over the Right MT+ on the FLE

Participants.

A total of 45 new participants were recruited to assign into three experimental groups: anodal group (aged 19–27 yr, mean 22.0 ± 2.9 yr; 9 females; 4 left-dominated eye; all right-handedness), cathodal group (aged 19–27 yr, mean 20.0 ± 2.9 yr; 7 females; 8 left-dominated eye; all right-handedness), and sham group (aged 18–26 yr, mean 21.3 ± 2.8 yr; 9 females; 7 left-dominated eye; 1 left-handedness), whose general characteristics were the same as those in *experiment 1*.

Transcranial direct current stimulation.

tDCS parameters were the same as those in *experiment 1*, except that the left MT+ was replaced by the right MT+ .

The flash-lag task.

We used the same apparatus, stimuli, and procedure as used in *experiment 1*.

Study protocol.

The protocol was as in *experiment 1* (Fig. 1*C*), except that, for the sham group, the electrode positions on eight participants were placed over the same sites as in the anodal group, and the electrode positions on seven participants were the same sites as in the cathodal group, which makes a counterbalance

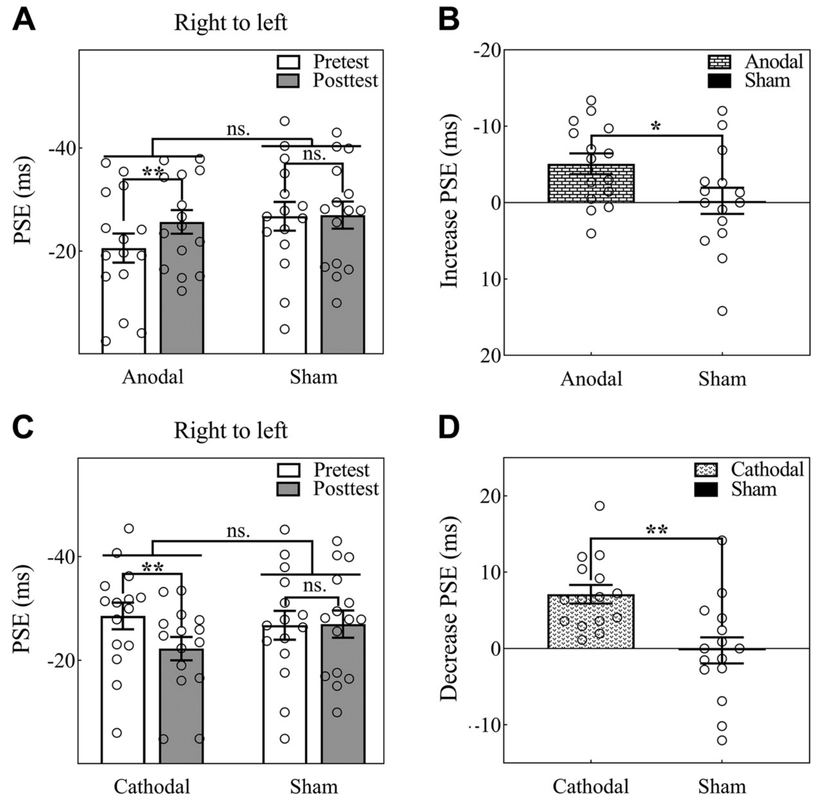

Figure 4. Increase and decrease effects of transcranial direct current stimulations (tDCS) over the left MT+ on the flash-lag effect (FLE) in the right to the left (RL) motion direction. *A*: increased effect of anodal (a)-tDCS. The pretest point of subjective equality (PSE) is significantly higher than the posttest PSE in the anodal group; the pretest PSE is nearly equal to the posttest PSE in the sham group. *B*: an comparison of the increased effect between the anodal and sham groups. The increased effect improvement is defined as (the posttest PSE − the pretest PSE), and the increased effect in the anodal group is significantly higher than that in the sham group. *C*: decreased effect of cathodal (c)-tDCS. The pretest PSE is significantly lower than the posttest PSE in the cathodal group; the pretest PSE is nearly equal to the posttest PSE in the sham group. *D*: an comparison of the decreased effect between the cathodal and sham groups. The decreased effect improvement is defined as (the posttest PSE − the pretest PSE), and the decreased effect in the anodal group is significantly higher than that in the sham group. Hollow circles represent individual points in each group. $*P < 0.05$, $**P < 0.01$; ns, nonsignificant.

on the electrode position number in two sham groups in two experiments. In addition, the current electrical field (V/m) created by the montage targeting the right MT+ is shown in Fig. 2, *right*.

Data processing and analysis.

We used the same data processing and analysis as in *experiment 1*.

Results.

To estimate the effects of tDCS on the right MT+ on the FLE in different motion directions, we performed a 2 (testing: pretest vs. posttest) × 2 [motion direction: the right to the left (RL) versus the left to the right (LR)] repeated-measures ANOVA with the PSE as the dependent measure in anodal, cathodal, and sham groups, respectively (see Supplemental Material). For the anodal group, we observed a significant main effect of testing ($F_{1,14} = 5.39$, $P < 0.05$, $\eta_p^2 = 0.28$) and testing × motion direction interaction effect ($F_{1,14} = 7.77$, $P < 0.05$, $\eta_p^2 = 0.36$) (Fig. 4*A*). A simple interaction analysis indicated that the posttest PSE was lower than the pretest PSE in the LR motion direction ($t_{14} = 5.30$, $P < 0.01$, Cohen's $d = 0.54$) (Fig. 5*A*). For the cathodal group, we observed a significant main effect of testing ($F_{1,14} = 8.61$, $P < 0.05$, $\eta_p^2 = 0.38$) and testing × motion direction interaction effect ($F_{1,14} = 14.11$, $P < 0.01$, $\eta_p^2 = 0.50$) (Fig. 5*B*). A simple interaction analysis indicated that the pretest PSE was lower than the posttest PSE in the LR motion direction ($t_{14} = 5.12$, $P < 0.01$, Cohen's $d = 0.81$) (Fig. 5*B*). For the sham group, no other significant results were found (Fig. 5*C*). For three groups, the JNDs did not significantly differ between different testings and motion directions (see Supplemental Fig. S2).

After the normalization of pre- and posttest PSEs in the LR motion direction, we run a 2 (testing: pretest vs. posttest) × 2 (stimulation: anodal vs. cathodal versus sham) repeated-measures ANOVA with the normalized PSE as the dependent measure. We observed a significant testing × stimulation interaction effect ($F_{2,42} = 11.00$, $P < 0.01$, $\eta_p^2 = 0.34$) (Fig. 5*D*). A simple interaction analysis (Bonferroni correction) indicated that the normalized pretest PSE was higher than the normalized posttest PSE in the anodal stimulation ($t_{42} = 2.16$, $P < 0.05$, Cohen's $d = 0.57$), the normalized pretest PSE was lower than the normalized posttest PSE in the cathodal stimulation ($t_{42} = 4.37$, $P < 0.001$, Cohen's $d = 1.15$), with no other significant results found (Fig. 5*D*).

To further verify the increased effect of tDCS on the FLE in the RL motion direction, we run a 2 (testing: pretest vs. posttest, within-group) × 2 (stimulation: anodal vs. sham, between-group) mixed-model ANOVA with the PSE as the dependent measure (49). We observed a marginally significant testing × stimulation interaction effect ($F_{1,28} = 3.47$, $P = 0.073$, $\eta_p^2 = 0.11$) (Fig. 6*A*). A simple effect analysis indicated that the pretest PSE was higher than the posttest PSE in the anodal stimulation ($t_{28} = 2.61$, $P = 0.015 < 0.05$, Cohen's $d = 0.69$), and no other significant results were found. Furthermore, we compared the discrepancy of the increased effect between anodal and sham groups. The increase in PSE (posttest − pretest) was estimated via the independent sample t test (two-tailed), with the result indicating that the increased effect in the anodal group was marginally more than that in the sham group ($t_{28} = 1.86$, $P = 0.073$, Cohen's $d = 0.68$) (Fig. 6*B*). Likewise, we further confirmed the decreased effect of tDCS on the FLE in the LR motion direction, we run a 2 (testing: pretest vs. posttest, within-group) × 2 (stimulation: cathodal vs. sham, between-

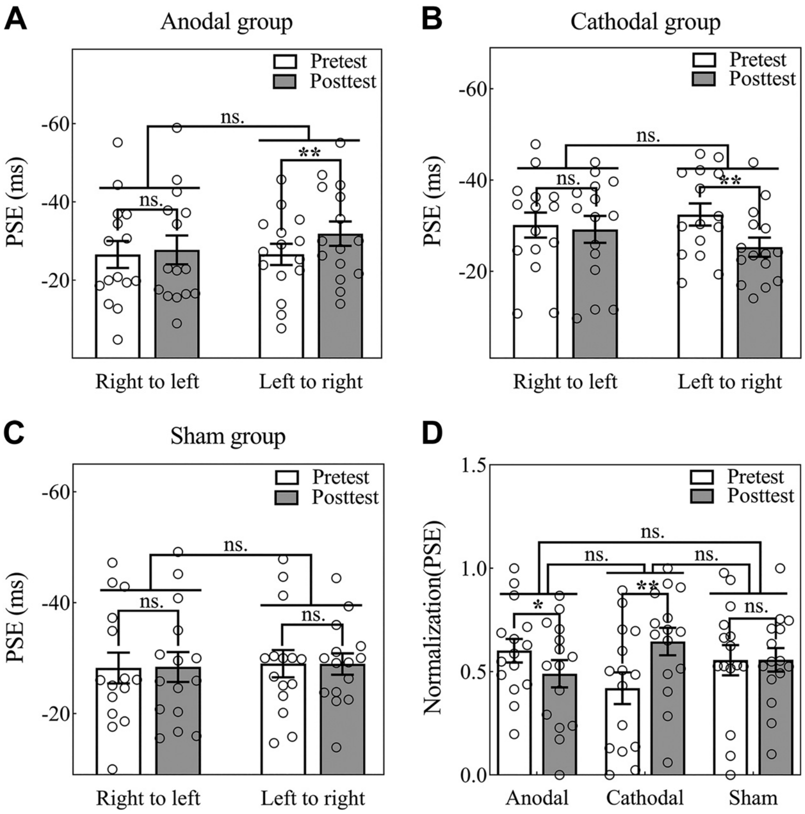

Figure 5. Effects of transcranial direct current stimulations (tDCS) over the right MT+ on the flash-lag effect (FLE) in different motion directions. *A*: effects of anodal (a)-tDCS. The pretest point of subjective equality (PSE) is near equal to the posttest PSE in the right to the left (RL) motion direction; the pretest PSE is significantly higher than the posttest PSE in the left to the right (LR) motion direction; the pretest PSE in the RL motion direction is nearly equal to that in the LR motion direction; the posttest PSE in the RL motion direction is nearly equal to that in the LR motion direction. *B*: effects of cathodal (c)-tDCS. The pretest PSE is nearly equal to the posttest PSE in the RL motion direction; the pretest PSE is significantly lower than the posttest PSE in the LR motion direction; the pretest PSE in the RL motion direction is nearly equal to that in the LR motion direction; the posttest PSE in the RL motion direction is nearly equal to that in the LR motion direction. *C*: effects of sham tDCS; there are no significant results; the test PSEs are nearly equal. *D*: effects of tDCS over the right MT+ on the FLE in the RL motion direction. To avoid the individual difference and better verify the effects of tDCS on the FLE in the LR motion direction, we normalized pre- and posttests of the PSE in each group using a min-max normalization method. The normalized pre- and posttests of the PSE in three types of stimulations do not significantly differ, respectively; in the anodal stimulation, the normalized pretest PSE is significantly higher than the normalized posttest PSE; in the cathodal stimulation, the normalized pretest PSE is significantly lower than the normalized posttest PSE. Hollow circles represent individual points in each group. *$P < 0.05$, **$P < 0.01$; ns, nonsignificant.

group) mixed-model ANOVA with the PSE as the dependent measure. We observed a significant testing × stimulation interaction effect ($F_{1,28} = 6.68$, $P < 0.05$, $\eta_p^2 = 0.20$) (Fig. 6*C*). A simple effect analysis indicated that the pretest PSE was lower than the posttest PSE in the cathodal stimulation ($t_{28} = 3.71$, $P < 0.001$, Cohen's $d = 0.98$), and no other significant results were found. Furthermore, we compared the discrepancy of the decreased effect between cathodal and sham groups. The decrease in PSE (posttest − pretest) was estimated via the independent sample *t* test (two-tailed), with the result indicating that the decreased effect in the cathodal group was more than that in the sham group ($t_{28} = 2.60$, $P < 0.05$, Cohen's $d = 0.95$) (Fig. 6*D*).

DISCUSSION

We assessed how tDCS over the left and right MT+ modulates the FLE in both the RL and LR motion directions. Our main finding is that after 15-min tDCS on the left MT+, a- and c-tDCS enhanced and reduced the magnitude of the FLE in the RL motion direction (Figs. 3 and 4), respectively, that after 15-min tDCS on the right MT+, a- and c-tDCS enhanced and reduced the magnitude of the FLE in the LR motion direction (Figs. 5 and 6), respectively, and that sham tDCS did not affect the magnitude of FLE in both the RL and LR motion directions (Fig. 3*C* and Fig. 5*C*). We suggest that a- and c-tDCS over the left and right MT+ can facilitate and inhibit the FLE with the moving bar heading to but not deviating from the side of the brain stimulated, respectively, compared with sham tDCS. These findings may help contribute to understanding the neural mechanism of the FLE.

We found that when a-tDCS was on the left MT+, the magnitude of the FLE in the RL motion direction increased (Fig. 3, *A* and *D* and Fig. 4, *A* and *B*), and when a-tDCS was on the right MT+, the magnitude of the FLE in the LR motion direction increased (Fig. 5, *A* and *D* and Fig. 6, *A* and *B*). One directional explanation for this result is that a-tDCS might increase the cortical excitability in MT+ (32, 33, 36), which might shift the perceptual localization of the moving bar toward the side of the brain stimulated when a flash appears. As it affected the PSE but not the JND (slope, the speed discrimination threshold), a-tDCS did not affect the subjects' speed discrimination ability but more likely introduced a perceptual decision bias in conditions of high uncertainty (e.g., a flash physically aligned with the moving bar), which may occur in MT+ fundamentally computing motion processing (33, 50). Furthermore the total activity of a subpopulation of MT+ neurons that tuned to the target direction proportionally scales the perceived speed (51, 52), thus a-tDCS on unilateral MT+ possibly causes an increase in the perceived speed of the moving bar toward the side stimulated (53), which enhances the magnitude of the FLE that is proportional to the perceived speed of the moving bar (4, 16). Alternatively, a-tDCS on unilateral MT+ might impose top-down feedback to the primary visual cortex (V1) coding position processing (54, 55), which indirectly influences the "perceived position" of the moving bar (not its perceived speed) toward the side stimulated.

We also found that when c-tDCS was on the left MT+, the magnitude of the FLE in the RL motion direction decreased (Fig. 3, *B* and *D* and Fig. 4, *C* and *D*), and when c-tDCS was on the right MT+, the magnitude of the FLE in the LR motion

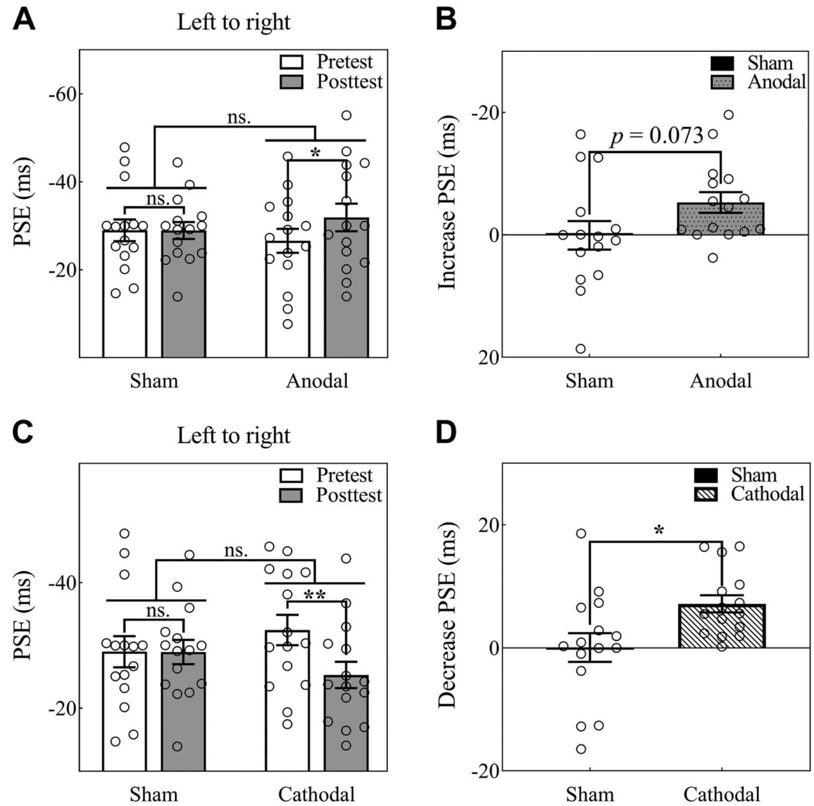

Figure 6. Increase and decrease effects of transcranial direct current stimulations (tDCS) over the right MT+ on the flash-lag effect (FLE) in the left to the right (LR) motion direction. *A*: increased effect of anodal (a)-tDCS. The pretest point of subjective equality (PSE) is significantly higher than the posttest PSE in the anodal group; the pretest PSE is nearly equal to the posttest PSE in the sham group. *B*: an comparison of the increased effect between the anodal and sham groups. The increased effect improvement is defined as (the posttest PSE − the pretest PSE), and the increased effect in the anodal group is marginally higher than that in the sham group. *C*: the decreased effect of cathodal (c)-tDCS. The pretest PSE is significantly lower than the posttest PSE in the cathodal group; the pretest PSE is nearly equal to the posttest PSE in the sham group. *D*: an comparison of the decreased effect between the cathodal and sham groups. The decreased effect improvement is defined as (the posttest PSE − the pretest PSE), and the decreased effect in the anodal group is significantly higher than that in the sham group. Hollow circles represent individual points in each group. *$P < 0.05$, **$P < 0.01$, ns, nonsignificant.

direction decreased (Fig. 5, *B* and *D* and Fig. 6, *C* and *D*). A similar explanation for this result is that the cathodal stimulation might decrease the cortical excitability in MT+ (32, 33, 35), which might shift the perceptual localization of the moving bar away from the side of the brain stimulated when a flash appears. Since c-tDCS also affected the PSE but not the JND, it may also introduce a perceptual decision bias in MT+ (50). Furthermore, c-tDCS on unilateral MT+ possibly decreased the total activity of a subpopulation of MT+ neurons (tuned to target direction), thereby leading to a decrease in the perceived speed of the moving bar toward the side stimulated, which reduces the magnitude of the FLE. Alternatively, c-tDCS on unilateral MT+ might impose top-down feedback to V1, which indirectly influences the "perceived position" of the moving bar away from the side stimulated.

Although our results clearly showed that the current stimulation of MT+ modulates the magnitude of the FLE, the identification of the mechanisms through which tDCS affects visual motion perception still requires further discussion. Indeed, tDCS can enhance and decrease cortical excitability in MT+ (30, 33, 35, 38). Interestingly, the modulation mechanisms of tDCS on motion perception may be different as visual motion task changes (33, 37). In our study, although the moving bar is easy to detect, a-tDCS, by increasing the probability of the firing rate, may activate more neurons tuned to the moving bar (56, 57). In particular, even those that originally do not reach the activation in the absence of stimulation may excite as a result of a-tDCS. Hence, a-tDCS might result in temporarily more neurons being activated to represent the moving bar, thereby overestimating the perceived speed of the moving bar than that in no stimulation (53, 58). Conversely, c-tDCS may depress those neurons tuning to the moving bar and attenuate the moving bar representation, thereby underestimating the perceived speed of the moving bar (52, 58). Alternatively, tDCS may modulate the top-down feedback from MT+ to V1, which biases the position coding in V1 and then induces perceived position shift due to motion perception (4, 10, 59, 60). One possibility is that the change of perceived position shift in V1 is attributable to the strength of motion processing in MT+ due to tDCS (4, 59); the other possibility is that the connectivity efficacy from MT+ to V1 might be mediated by tDCS, which causes the change of perceived position shift (3, 9).

In addition, our findings have implications for spatial mechanisms for the FLE, although the present study was not designed to falsify one of the various mechanism interpretations. Spatial mechanisms explain the FLE as a predictive forward shift of the moving object, potentially compensating for the transmission delays of the visual signal from the eye to the visual cortex (4, 6, 8). Indeed, predictable motion preactivates the future positions of moving objects and attenuated the neural response to objects moving into a predictive region (6, 61, 62). Thus, perceptual position shifts are thought to be the result of an interaction of lateral inhibition and excitation in retinotopic maps and/or feedback from the higher areas. Furthermore, modifying neural activity in MT+ might directly interfere with perceived motion and/or feedback signals, which would usually change a misalignment in the motion direction.

Also, our results did not well distinguish the pre- and post-flashed stimulus-dependent temporal processings in the FLE. Interestingly, tDCS did only affect the PSE but not the JND, indicating that tDCS might modulate the perceptual decision processing in the FLE, which indicates that early visual signals evoked by the moving bar are necessary for or correlated with the later decision processing (63). Although motion extrapolation or postdiction account did not separately interpret the current results, the modulation effect of tDCS on the FLE suggests that the later decision processing in MT+ likely imposes the top-down feedback to V1, affecting the perceived position of the moving bar. The agreement reconciles with one statement that the primary visual regions contralateral to the poststimulus movement are critical for the FLE (64). Therefore, the present findings suggest that tDCS might modulate the postflash decision processing in the FLE.

The FLE points out the significant difficulties that the visual system has while trying to correctly pinpoint the physical locations of moving objects. But the visual system attempts to correct the positional error by some neural mechanisms, which made psychophysical outcomes on the FLE multifaceted and complicated. Therefore, the modulation effects of tDCS over MT+ on the FLE require further verification in various flash-lag paradigms. In addition, we have to consider that modulation of the excitability in MT+ owing to tDCS is unlikely to only affect neuronal function in that targeted brain regions (36). Since the MT+-CZ montage with large disk electrodes allows for ample current spread, it cannot be completely ruled out a possibility that other motion-sensitive areas (such as region V3A/V3), were also activated (35), which possibly modulates the FLE.

SUPPLEMENTAL DATA

Supplemental Material: https://doi.org/10.6084/m9.figshare.19187522.v1.

GRANTS

This work was supported by grants from Natural Science Foundation of China (T2192932, 62061136001), and the Ministry of Science and Technology of China (2021ZD0202601).

DISCLOSURES

No conflicts of interest, financial or otherwise, are declared by the authors.

AUTHOR CONTRIBUTIONS

W.W. and L.C. conceived and designed research; W.W., X.L., and K.L. performed experiments; W.W. analyzed data; W.W., X.L., W.G., and K.L. interpreted results of experiments; W.W. prepared figures; W.W. drafted manuscript; W.W. and L.C. edited and revised manuscript; W.W., X.L., W.G., and L.C. approved final version of manuscript.

ENDNOTE

At the request of the authors, readers are herein alerted to the fact that additional materials related to this manuscript may be found at https://doi.org/10.6084/m9.figshare.19187522.v1. These materials are not a part of this manuscript and have not undergone peer review by the American Physiological Society (APS). APS and the journal editors take no responsibility for these materials, for the website address, or for any links to or from it.

REFERENCES

1. **Baldo MVC**, **Ranvaud RD**, **Morya E.** Flag errors in soccer games: the flash-lag effect brought to real life. *Perception* 31: 1205–1210, 2002. doi:10.1068/p3422.
2. **Su J**, **Lu H.** Flash-lag effects in biological motion interact with body orientation and action familiarity. *Vision Res* 140: 13–24, 2017. doi:10.1016/j.visres.2017.06.010.
3. **Song Y**, **Wang H.** Motion-induced position mis-localization predicts the severity of Alzheimer's disease. *J Neuropsychol* 14: 333–345, 2020. doi:10.1111/jnp.12181.
4. **Maus GW**, **Ward J**, **Nijhawan R**, **Whitney D.** The perceived position of moving objects: transcranial magnetic stimulation of area MT+ reduces the flash-lag effect. *Cereb Cortex* 23: 241–247, 2013. doi:10.1093/cercor/bhs021.
5. **Khoei MA**, **Masson GS**, **Perrinet LU.** The flash-lag effect as a motion-based predictive shift. *PLoS Comput Biol* 13: e1005068, 2017. doi:10.1371/journal.pcbi.1005068.
6. **Hogendoorn H.** Motion extrapolation in visual processing: lessons from 25 years of flash-lag debate. *J Neurosci* 40: 5698–5705, 2020. doi:10.1523/JNEUROSCI.0275-20.2020.
7. **Nijhawan R.** Neural delays, visual motion and the flash-lag effect. *Trends Cogn Sci* 6: 387–393, 2002. doi:10.1016/S1364-6613(02)01963-0.
8. **Nijhawan R.** Visual prediction: psychophysics and neurophysiology of compensation for time delays. *Behav Brain Sci* 31: 179–239, 2008. doi:10.1017/S0140525X08003804.
9. **Ye F**, **Ye M**, **An J**, **Wang D**, **Wang Q**, **Chen Y**, **Peng X.** Motion-induced position shift in early Alzheimer's disease. *Sci Rep* 8: 9833, 2018. doi:10.1038/s41598-018-27991-0.
10. **Kohler PJ**, **Cavanagh P**, **Tse PU.** Motion-induced position shifts activate early visual cortex. *Front Neurosci* 11: 168, 2017. doi:10.3389/fnins.2017.00168.
11. **Baldo MVC**, **Kihara AH**, **Namba J**, **Klein SA.** Evidence for an attentional component of the perceptual misalignment between moving and flashing stimuli. *Perception* 31: 17–30, 2002. doi:10.1068/p3302.
12. **Baldo MVC**, **Klein SA.** Extrapolation or attention shift. *Nature* 378: 565–566, 1995. doi:10.1038/378565a0.
13. **Whitney D**, **Murakami I**, **Cavanagh P.** Illusory spatial offset of a flash relative to a moving stimulus is caused by differential latencies for moving and flashed stimuli. *Vision Res* 40: 137–149, 2000. doi:10.1016/S0042-6989(99)00166-2.
14. **Krekelberg B**, **Lappe M.** Neuronal latencies and the position of moving objects. *Trends Neurosci* 24: 335–339, 2001. doi:10.1016/S0166-2236(00)01795-1.
15. **Eagleman DM**, **Sejnowski TJ.** Motion integration and postdiction in visual awareness. *Science* 287: 2036–2038, 2000. doi:10.1126/science.287.5460.2036.
16. **Nijhawan. R.** Motion extrapolation in catching. *Nature* 370: 256–257, 1994. doi:10.1038/370256b0.
17. **Vroomen J**, **de Gelder B**, **Vroomen J.** Temporal ventriloquism: sound modulates the flash-lag effect. *J Exp Psychol Hum Percept Perform* 30: 513–518, 2004. doi:10.1037/0096-1523.30.3.513.
18. **Eagleman DM**, **Sejnowski TJ.** Motion signals bias localization judgments: a unified explanation for the flash-lag, flash-drag, flash-jump, and Frohlich illusions. *J Vis* 7: 3–12, 2007. doi:10.1167/7.4.3.
19. **Fischer J**, **Spotswood N**, **Whitney D.** The emergence of perceived position in the visual system. *J Cogn Neurosci* 23: 119–136, 2011. doi:10.1162/jocn.2010.21417.
20. **Kolster H**, **Peeters R**, **Orban GA.** The retinotopic organization of the human middle temporal area MT/V5 and its cortical neighbors. *J Neurosci* 30: 9801–9820, 2010. doi:10.1523/JNEUROSCI.2069-10.2010.
21. **Moo LR**, **Emerton BC**, **Slotnick SD.** Functional MT+ lesion impairs contralateral motion processing. *Cogn Neuropsychol* 25: 677–689, 2008. doi:10.1080/02643290802271599.
22. **Strong SL**, **Silson EH**, **Gouws AD**, **Morland AB**, **Mckeefry DJ.** An enhanced role for right hV5/MT+ in the analysis of motion in the contra- and ipsi-lateral visual hemi-fields. *Behav Brain Res* 372: 112060, 2019. doi:10.1016/j.bbr.2019.112060.
23. **Walsh V**, **Ellison A**, **Battelli L**, **Cowey A.** Task-specific impairments and enhancements induced by magnetic stimulation of human visual area V5. *Proc Biol Sci* 265: 537–543, 1998. doi:10.1098/rspb.1998.0328.

24. **Thompson B**, **Deblieck C**, **Wu A**, **Iacoboni M**, **Liu Z.** Brain stimulation psychophysical and rTMS evidence for the presence of motion opponency in human V5. *Brain Stimul* 9: 876–881, 2016. doi:10.1016/j.brs.2016.05.012.
25. **Zinchenko A**, **Brunner S**, **Chen L**, **Shi Z**, **Paul C**, **Taylor J**, **Müller HJ.** V5/MT+ modulates spatio-temporal integration differently across and within hemifields: causal evidence from TMS. *Neuropsychologia* 161: 107995, 2021. doi:10.1016/j.neuropsychologia.2021.107995.
26. **Thakral PP**, **Slotnick SD.** Disruption of MT impairs motion processing. *Neurosci Lett* 490: 226–230, 2011. doi:10.1016/j.neulet.2010.12.057.
27. **Akin B**, **Ozdem C**, **Eroglu S**, **Keskin DT**, **Fang F**, **Doerschner K**, **Kersten D**, **Boyaci H.** Attention modulates neuronal correlates of interhemispheric integration and global motion perception. *J Vis* 14: 30, 2014. doi:10.1167/14.12.30.
28. **Amano K**, **Wandell BA**, **Dumoulin SO.** Visual field maps, population receptive field sizes, and visual field coverage in the human MT+ complex. *J Neurophysiol* 102: 2704–2718, 2009. doi:10.1152/jn.00102.2009.
29. **Huk AC**, **Dougherty RF**, **Heeger DJ.** Retinotopy and functional subdivision of human areas MT and MST. *J Neurosci* 22: 7195–7205, 2002. doi:10.1523/JNEUROSCI.22-16-07195.2002.
30. **McGraw PV**, **Walsh V**, **Barrett BT.** Motion-sensitive neurones in V5/MT modulate perceived spatial position. *Curr Biol* 14: 1090–1093, 2004. doi:10.1016/j.cub.2004.06.028.
31. **Whitney D**, **Ellison A**, **Rice NJ**, **Arnold D**, **Goodale M**, **Walsh V**, **Milner D.** Visually guided reaching depends on motion area MT+. *Cereb Cortex* 17: 2644–2649, 2007. doi:10.1093/cercor/bhl172.
32. **Antal A**, **Nitsche MA**, **Paulus W.** Transcranial direct current stimulation and the visual cortex. *Brain Res Bull* 68: 459–463, 2006. doi:10.1016/j.brainresbull.2005.10.006.
33. **Battaglini L**, **Noventa S**, **Casco C.** Anodal and cathodal electrical stimulation over V5 improves motion perception by signal enhancement and noise reduction. *Brain Stimul* 10: 773–779, 2017. doi:10.1016/j.brs.2017.04.128.
34. **Bestmann S**, **de Berker AO**, **Bonaiuto J.** Understanding the behavioural consequences of noninvasive brain stimulation. *Trends Cogn Sci* 19: 13–20, 2015. doi:10.1016/j.tics.2014.10.003.
35. **Antal A**, **Nitsche MA**, **Kruse W**, **Kincses TZ**, **Hoffmann KP**, **Paulus W.** Direct current stimulation over V5 enhances visuomotor coordination by improving motion perception in humans. *J Cogn Neurosci* 16: 521–527, 2004. doi:10.1162/089892904323057263.
36. **Antal A**, **Nitsche MA**, **Kincses TZ**, **Kruse W**, **Hoffmann KP**, **Paulus W.** Facilitation of visuo-motor learning by transcranial direct current stimulation of the motor and extrastriate visual areas in humans. *Eur J Neurosci* 19: 2888–2892, 2004. doi:10.1111/j.1460-9568.2004.03367.x.
37. **Miniussi C**, **Harris JA**, **Ruzzoli M.** Modelling non-invasive brain stimulation in cognitive neuroscience. *Neurosci Biobehav Rev* 37: 1702–1712, 2013. doi:10.1016/j.neubiorev.2013.06.014.
38. **Antal A**, **Varga ET**, **Nitsche MA**, **Chadaide Z**, **Paulus W**, **Kovács G**, **Vidnyánszky Z.** Direct current stimulation over MT+/V5 modulates motion aftereffect in humans. *Neuroreport* 15: 2491–2494, 2004. doi:10.1097/00001756-200411150-00012.
39. **Pelli DG.** The VideoToolbox software for visual psychophysics: transforming numbers into movies. *Spat Vis* 10: 437–442, 1997.
40. **Brainard DH.** The psychophysics toolbox. *Spat Vis* 10: 433–436, 1997. doi:10.1163/156856897X00357.
41. **Huang Y**, **Datta A**, **Bikson M**, **Parra LC.** ROAST: an open-source, fully-automated, realistic volumetric-approach-based simulator for TES. *Annu Int Conf IEEE Eng Med Biol Soc* 2018: 3072–3075, 2018. doi:10.1109/EMBC.2018.8513086.[30441043]
42. **Huang Y**, **Datta A**, **Bikson M**, **Parra LC.** Realistic volumetric-approach to simulate transcranial electric stimulation—ROAST—a fully automated open-source pipeline. *J Neural Eng* 16: 056006, 2019. doi:10.1088/1741-2552/ab208d.
43. **Liu Y**, **Yang J**, **Yu Y**, **Yu Y**, **Wang W**, **Li H**, **Takahashi S**, **Ejima Y**, **Wu Q**, **Wu J.** A new method for haptic shape discriminability detection. *Appl Sci* 11: 1–19, 2021. doi:10.3390/app11157049.
44. **Wang W**, **Yang J**, **Yu Y**, **Wu Q**, **Yu J**, **Takahashi S**, **Ejima Y**, **Wu J.** Tactile angle discriminability improvement: Roles of training time intervals and different types of training tasks. *J Neurophysiol* 122: 1918–1927, 2019. doi:10.1152/jn.00161.2019.
45. **Wang W**, **Yang J**, **Yu Y**, **Li H**, **Liu Y**, **Yu Y**, **Yu J**, **Tang X**, **Yang J**, **Takahashi S**, **Ejima Y**, **Wu J.** Tactile angle discriminability improvement: contributions of working memory training and continuous attended sensory input. *J Neurophysiol* 127: 1398–1406, 2022. doi:10.1152/jn.00529.2021.
46. **Wang W**, **Yang J**, **Yu Y**, **Wu Q**, **Takahashi S**, **Ejima Y**, **Wu J.** Tactile semiautomatic passive-finger angle stimulator (TSPAS). *J Vis Exp* 161: e61218, 2020. doi:10.3791/61218.
47. **Bao H-W-S.** bruceR: broadly useful convenient and efficient R functions (Online). https://cran.r-project.org/package=bruceR [2022 Jul 3].
48. **Jain A**, **Nandakumar K**, **Ross A.** Score normalization in multimodal biometric systems. *Pattern Recognit* 38: 2270–2285, 2005. doi:10.1016/j.patcog.2005.01.012.
49. **Nieuwenhuis S**, **Forstmann BU**, **Wagenmakers EJ.** Erroneous analyses of interactions in neuroscience: a problem of significance. *Nat Neurosci* 14: 1105–1107, 2011. doi:10.1038/nn.2886.
50. **Battaglini L.** Effect of repetitive transcranial magnetic stimulation on a target moving in front of a static or random dynamic visual noise. *Perception* 49: 882–892, 2020. doi:10.1177/0301006620940222.
51. **Krekelberg B**, **Wezel RV**, **Albright TD.** Interactions between speed and contrast tuning in the middle temporal area: implications for the neural code for speed. *J Neurosci* 26: 8988–8998, 2006. doi:10.1523/JNEUROSCI.1983-06.2006.
52. **McKeefry DJ**, **Burton MP**, **Vakrou C**, **Barrett BT**, **Morland AB.** Induced deficits in speed perception by transcranial magnetic stimulation of human cortical areas V5/MT+ and V3A. *J Neurosci* 28: 6848–6857, 2008. doi:10.1523/JNEUROSCI.1287-08.2008.
53. **Komatsu H**, **Wurtz RH.** Modulation of pursuit eye movements by stimulation of cortical areas MT and MST. *J Neurophysiol* 62: 31–47, 1989. doi:10.1152/jn.1989.62.1.31.
54. **Saenz M**, **Fine I.** Topographic organization of V1 projections through the corpus callosum in humans. *NeuroImage* 52: 1224–1229, 2010. doi:10.1016/j.neuroimage.2010.05.060.
55. **Laycock R**, **Crewther DP**, **Fitzgerald PB**, **Crewther SG.** Evidence for fast signals and later processing in human V1/V2 and V5/MT+: a TMS study of motion perception. *J Neurophysiol* 98: 1253–1262, 2007. doi:10.1152/jn.00416.2007.
56. **Jazayeri M**, **Movshon JA.** Integration of sensory evidence in motion discrimination. *J Vis* 7: 7.1–7.7, 2007. doi:10.1167/7.12.7.
57. **Hol K**, **Treue S.** Different populations of neurons contribute to the detection and discrimination of visual motion. *Vision Res* 41: 685–689, 2001. doi:10.1016/S0042-6989(00)00314-X.
58. **Boyraz P**, **Treue S.** Misperceptions of speed are accounted for by the responses of neurons in macaque cortical area MT. *J Neurophysiol* 105: 1199–1211, 2011. doi:10.1152/jn.00213.2010.
59. **Maus GW**, **Fischer J**, **Whitney D.** Motion-dependent representation of space in area MT+. *Neuron* 78: 554–562, 2013. doi:10.1016/j.neuron.2013.03.010.
60. **Fu YX**, **Shen Y**, **Gao H**, **Dan Y.** Asymmetry in visual cortical circuits underlying motion-induced perceptual mislocalization. *J Neurosci* 24: 2165–2171, 2004. doi:10.1523/JNEUROSCI.5145-03.2004.
61. **Schellekens W**, **van Wezel RJA**, **Petridou N**, **Ramsey NF**, **Raemaekers M.** Predictive coding for motion stimuli in human early visual cortex. *Brain Struct Funct* 221: 879–890, 2016. doi:10.1007/s00429-014-0942-2.
62. **Hogendoorn H**, **Burkitt AN.** Predictive coding of visual object position ahead of moving objects revealed by time-resolved EEG decoding. *NeuroImage* 171: 55–61, 2018. doi:10.1016/j.neuroimage.2017.12.063.
63. **Sergent C.** The offline stream of conscious representations. *Philos Trans R Soc B Biol Sci* 373, 2018. doi:10.1098/rstb.2017.0349.
64. **Keil J**, **Senkowski D**, **Moran JK.** Early and late evoked brain responses differentially reflect feature encoding and perception in the flash-lag illusion. *NeuroImage* 246: 118787, 2022. doi:10.1016/j.neuroimage.2021.118787.